Journal of Power Sources 196 (2011) 5631–5636

Contents lists available at ScienceDirect

Journal of Power Sources

journal homepage: www.elsevier.com/locate/jpowsour

Gallium (III) sulfide as an active material in lithium secondary batteries

Hiroshi Senoh[a,*], Hiroyuki Kageyama[a], Tomonari Takeuchi[a], Koji Nakanishi[b], Toshiaki Ohta[b], Hikari Sakaebe[a], Masaru Yao[a], Tetsuo Sakai[a], Kazuaki Yasuda[a]

[a] Research Institute for Ubiquitous Energy Devices, National Institute of Advanced Industrial Science and Technology (AIST), 1-8-31 Midorigaoka, Ikeda, Osaka 563-8577, Japan
[b] Synchrotron Radiation Center (The SR Center), Ritsumeikan University, 1-1-1 Noji-Higashi, Kusatsu, Shiga 525-8577, Japan

ARTICLE INFO

Article history:
Received 15 December 2010
Received in revised form 14 February 2011
Accepted 17 February 2011
Available online 26 February 2011

Keywords:
Lithium secondary battery
Gallium (III) sulfide
Capacity retention
Rate capability
X-ray diffraction
X-ray absorption fine structure

ABSTRACT

In an attempt to identify an active material for use in lithium secondary batteries with high energy density, we investigated the electrochemical properties of gallium (III) sulfide (Ga_2S_3) at 30 °C. Ga_2S_3 shows two sloping plateaus in the potential range between 0.01 V and 2.0 V vs. (Li/Li^+). The specific capacity of the Ga_2S_3 electrode in the first delithiation is ca. 920 mAh g^{-1}, which corresponds to 81% of the theoretical capacity (assuming a 10-electron reaction). The capacity in the 10th cycle is 63% of the initial capacity. *Ex situ* X-ray diffraction and X-ray absorption fine structure analyses revealed that the reaction of the Ga_2S_3 electrode proceeds in two steps: $Ga_2S_3 + 6Li^+ + 6e^- \leftrightarrows 2Ga + 3Li_2S$ and $Ga + xLi^+ + xe^- \leftrightarrows Li_xGa$.

1. Introduction

Lithium secondary batteries have been widely used because of their high energy characteristics. Various active materials have been proposed as novel electrodes. Sulfur is a promising active material because of its high theoretical capacity and relatively low cost [1]. To circumvent the limitations of sulfur (low electronic conductivity and a tendency to dissolve into the electrolyte), many attempts have been made to alloy sulfur with a metal to form a sulfide. A variety of transition metal-containing sulfides, such as FeS_2, NiS_2 and CuS, have been studied for use as cathode active materials [2–4].

Recently, some sulfides of *p*-block elements have been proposed as anode active materials [5–7]. For example, Kim et al. reported that a GeS_2 glass could serve as a new class of anode material because of its high Li^+ conductivity [5]. Hang et al. investigated the electrochemical properties of Li_2SiS_3 in a solid electrolyte and found that Li_2SiS_3 has a large capacity with small capacity degradation [6]. Quite recently, we found that a sulfide of an earth metal – aluminum sulfide (Al_2S_3) – has high specific capacity in the potential range between 0.01 V and 2.0 V vs. (Li/Li^+) [7].

In this study, we focused on another sulfide of an earth metal – gallium (III) sulfide (Ga_2S_3) – for use as an anode active material. Ga_2S_3 is a component of lithium-containing sulfide glass, which has been studied as a possible solid-state electrolyte material for use in lithium secondary batteries [8–10]. To our knowledge, there has been no previous report on the possible application of Ga_2S_3 as an anode material in lithium secondary batteries. If the complete lithiation of Ga_2S_3 is assumed ($Ga_2S_3 + 10Li^+ + 10e^- \leftrightarrows 2Li_2Ga + 3Li_2S$), the theoretical capacity would be 1137 mAh g^{-1}. This value is about three times as large as that of the conventional active material – graphite. In the present study, we examined the electrochemical properties of Ga_2S_3, and focused on its structural changes by means of *ex situ* X-ray diffraction and X-ray absorption fine structure analyses to understand the reaction mechanisms during galvanostatic cycles.

2. Experimental

Commercially available Ga_2S_3 powder (Kojundo Chemical Laboratory Co., Ltd., 99.99%) was used as-received for the electrochemical studies. SEM observation revealed that the Ga_2S_3 powder was composed of flaky particles of 2–3 μm in size. A slurry to form the working electrode was prepared by mixing the Ga_2S_3 powder, ketchen black as a conductive additive, and polyimide as a binder in a weight ratio of 80:5:15 in *N*-methyl-2-pyrrolidone. The prepared slurry was loaded onto copper foil as a current collector. The resultant electrode was dried and then roll-pressed to a thickness of about 60 μm. The electrode was heated at 300 °C for 1 h under vacuum to give stronger bonding between the anode material and the

* Corresponding author. Tel.: +81 72 751 9612; fax: +81 72 751 9629.
E-mail address: h.senoh@aist.go.jp (H. Senoh).

0378-7753/$ – see front matter © 2011 Elsevier B.V. All rights reserved.
doi:10.1016/j.jpowsour.2011.02.054

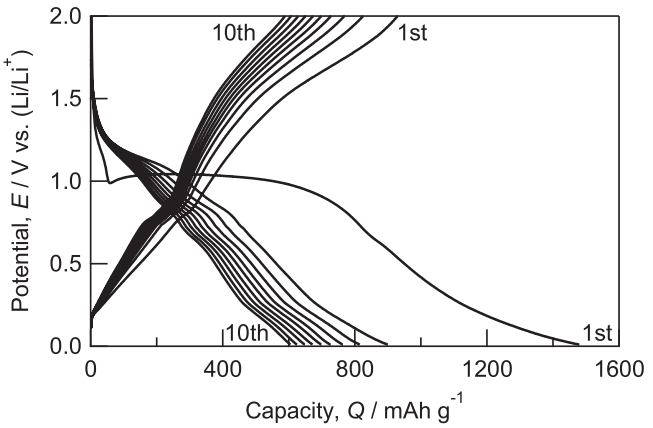

Fig. 1. Potential profiles of a Ga_2S_3 electrode in the 1st to 10th cycles.

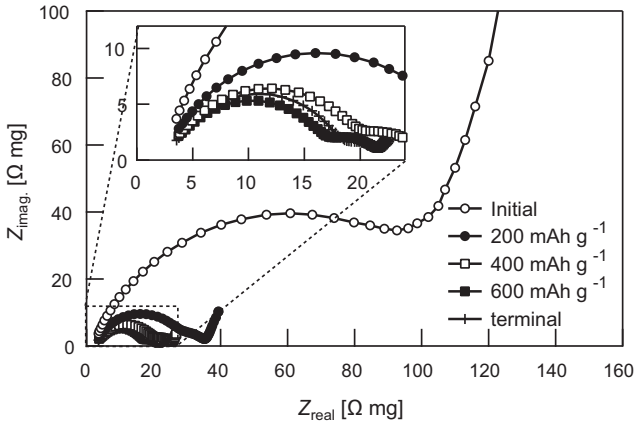

Fig. 2. Electrochemical impedance spectra of a Ga_2S_3 electrode during the 1st lithiation: initial, 200, 400, 600 mAh g^{-1} and terminal.

other materials. A blank electrode without Ga_2S_3 was also prepared at the same procedure.

A galvanostatic cycle test was performed in a half-cell (HS cell, Hohsen Corp.) constructed in an Ar-filled glove box. The counter electrode was Li foil (Honjo Metal Co., Ltd.). The separator was a porous polypropylene sheet (Asahi Kasei Chemicals Co., Ltd.). The electrolyte was 1 mol L^{-1} lithium hexafluorophosphate in a 1:1 mixture of ethylene carbonate and dimethyl carbonate (Kishida Chemical Co., Ltd.). The cycle test was conducted at 30 °C using a charge/discharge unit (ABE1024-05R1, Electrofield). In the cycle test, the prepared working electrode was first reduced (lithiated) at a current density of 100 mA g^{-1} with a cutoff potential of 0.01 V, allowed to rest for 1 h, and then oxidized (delithiated) at the same current density with a cutoff potential of 2.0 V unless otherwise stated. During the cycle test, the electrochemical impedance spectra of the cell were measured in the frequency range of 20 kHz to 0.1 Hz with a perturbation of 10 mV against a rest potential (SI1280B, Solartron Instruments).

After the cycle test, the cell was disassembled inside the Ar glove box and the working electrode was washed with dimethyl carbonate to remove the electrolyte. *Ex situ* X-ray diffraction (XRD) analysis of the electrode was performed under an Ar atmosphere by covering it with a polyimide film to avoid any reaction with moisture and air. The XRD patterns were recorded with an XRD unit (RINT-2500, Rigaku Corp.) using Cu Kα radiation at room temperature. Ga K-edge X-ray absorption fine structure (XAFS) analysis of the electrode, which was sealed in a laminate pack in an Ar atmosphere, was carried out in the transmission mode by using an X-ray spectrometer (EXAC-820, Technos Co., Ltd.) at room temperature. S K-edge XAFS analysis of the electrode was performed at BL-10 of the SR Center, Ritsumeikan University [11]. Samples were prepared in an Ar-filled glove box, transferred, and loaded in the XAFS sample chamber in vacuum without being exposed to air. XAFS spectra were obtained in both the total electron yield mode and the partial fluorescence yield mode.

3. Results

Potential profiles of the Ga_2S_3 electrode during the cycle test are shown in Fig. 1. Prior to reduction, no reaction of the Ga_2S_3 electrode was observed in the potential range of 2.0–4.0 V. The first reduction curve shows a large plateau at ca. 1.0 V. This is mainly attributed to lithiation of the Ga_2S_3 electrode, as mentioned later. A slight increase in the potential in the early stages of the plateau is due to a decrease in the overpotential induced by the reaction resistance. This is confirmed by the electrochemical impedance analysis (Fig. 2). The large impedance of the cell before reduction (Initial) drastically decreases in the early stages of the plateau, and thereafter the impedance changes slightly. Naturally, while other factors such as nucleation of the product affect the impedance, there is a drastic decrease in impedance only in the early stages of the first reduction. As shown in Fig. 1, during the first reduction, the potential gradually decreases after the large plateau, and another plateau appears below 0.3 V. The total reduction capacity (ca. 1450 mAh g^{-1}) is beyond the theoretical capacity. There are at least two possible explanations for this over-reduction: the formation of a solid–electrolyte interface (SEI), which uses extra electric current, and the contribution from the capacities of ketchen black and polyimide. In the subsequent first oxidation (delithiation), the potential increases gradually and the capacity of the electrode exceeds 900 mAh g^{-1}. Overall, two sloping plateaus appear during the lithiation process (ca. 1.1 V and below 0.3 V) as well as the delithiation process (ca. 0.8 V and 1.7 V). All of the plateau regions gradually become narrow with an increase in the cycle number.

Cycle performance in the delithiation capacity of Ga_2S_3 is shown in Fig. 3. The capacity contributions of the over-reduction from the SEI, ketchen black and polyimide were subtracted out by using the blank electrode. The first delithiation capacity of Ga_2S_3 is 920 mAh g^{-1}, which is 81% of the theoretical capacity. The capacity decreases more rapidly in the initial five cycles than in the subsequent cycles. The capacity at the 10th cycle is close to 600 mAh g^{-1} (capacity retention: 63%). This is superior to that of Al_2S_3, the capacity of which dropped to 240 mAh g^{-1} after 10 cycles [7] (although the preparation of Al_2S_3 electrode by mixing Al_2S_3 powder with teflonized acetylene black is different from that of Ga_2S_3 electrode

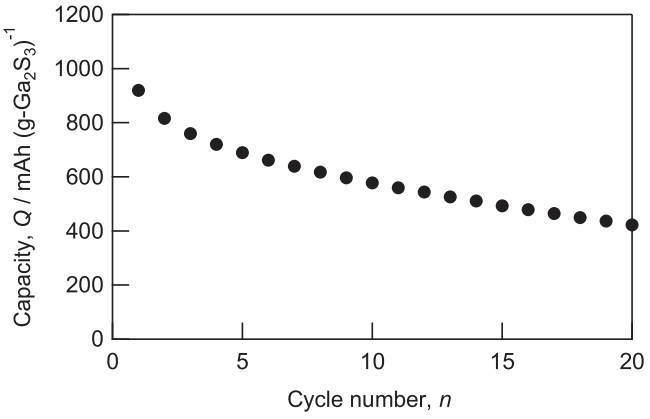

Fig. 3. Delithiation capacity of Ga_2S_3 at 100 mA g^{-1} corrected for the SEI, ketchen black and polyimide as a function of the cycle number.

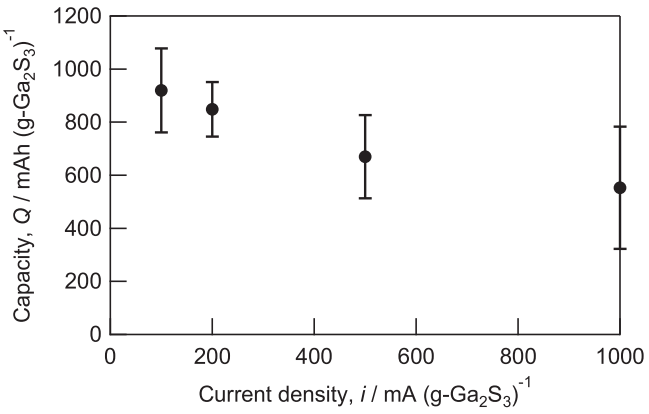

Fig. 4. Delithiation capacity of Ga_2S_3 at the 1st cycle corrected for the SEI, ketchen black and polyimide as a function of the current density. The error is twice of the standard deviation of the mean values.

in this study). The capacity observed during the lithiation process is comparable to that of the preceding delithiation capacity throughout the cycles. This suggests that the capacity mainly decreases during the delithiation process.

The rate capability of Ga_2S_3 is shown in Fig. 4. The delithiation capacity in the first cycle decreases linearly with an increase in the current density. Nonetheless, even at a current density of as high as 1000 mA g^{-1}, the delithiation capacity is still more than half of that at 100 mA g^{-1}. The large surface of the Ga_2S_3 powder, as noted in Section 2, plays an important role in the reaction of electrode material for high-rate utilization.

To clarify the reaction mechanism and the factors that underlie the degradation during cycling, XRD analysis was performed. The *ex situ* XRD profiles of the Ga_2S_3 electrode are shown in Fig. 5. For the prepared electrode before the cycle test (Initial in Fig. 5), all of the diffraction peaks are assigned to the α-Ga_2S_3 monoclinic structure [12]. After the first lithiation, some peaks corresponding to Li_2S [13] appear, while the diffraction peaks of Ga_2S_3 disappear. The material that underwent the first delithiation does not give a distinctive diffraction peak, but rather a broad hump at around 28–32° which is probably due to a nano-structured or amorphous state of Ga_2S_3. During the second lithiation, the intensities of the diffraction peaks of Li_2S increase again, and become almost identical to those after the first lithiation. The other peaks observed at 25.1°, 41.7° and 49.3°, which are quite small after the first lithiation can be assigned to LiGa [14]. These peaks were also observed more clearly after third lithiation. Li_2S remained even in the delithiation state after 10 cycles, while no other peaks attributable to phases in the Li–Ga–S system such as $LiGaS_2$ were observed.

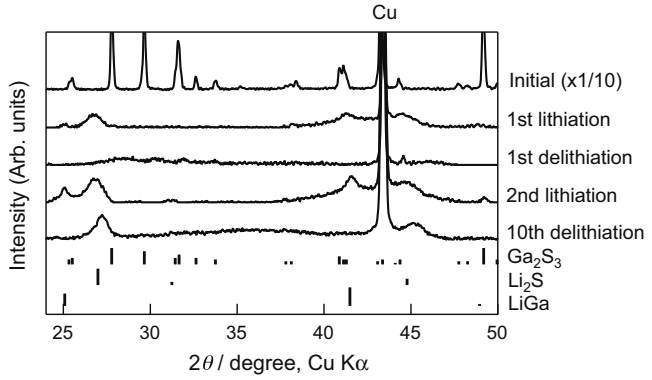

Fig. 5. *Ex situ* XRD profiles of a Ga_2S_3 electrode before and after the cycle test. Scan rate: 0.2° min^{-1}, scan step: 0.02°.

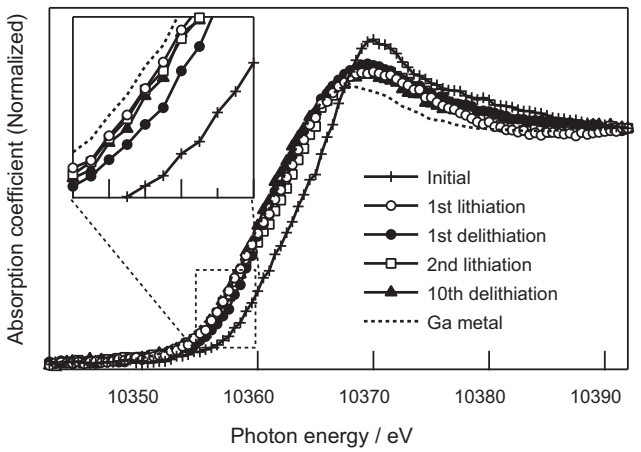

Fig. 6. Ga K-edge XANES spectra of a Ga_2S_3 electrode in the transmission mode before and after the cycle test. Ga metal was used as a reference. These spectra were normalized at 10392 eV.

The details of the structural changes were examined by Ga K-edge and S K-edge XFAS analyses. Fig. 6 shows the *ex situ* Ga K-edge X-ray absorption near edge structure (XANES) spectra of the Ga_2S_3 electrode measured in the transmission mode. The fact that the edge energy of Ga_2S_3 before the cycle (Initial) is at a higher position than that of metallic Ga indicates that Ga is, on average, in an oxidized state in Ga_2S_3. The average oxidation state of Ga decreases during the first lithiation, possibly due to the formation of Ga metal or Li–Ga alloy. The edge position then shifts slightly to a higher energy and the peak top is more enhanced. The reduction of Ga proceeds slightly during the cycles, as indicated by the differences in the edge positions after the first and 10th delithiation conditions. The lack of a significant change in the XANES spectra after the cycle test suggests that the oxidation state of Ga is not a practical variant, as expected during the cycle test.

The k^3-weighted extended X-ray absorption fine structure (EXAFS) oscillations of the Ga K-edge for a Ga_2S_3 electrode and the corresponding magnitude of the Fourier transforms are shown in Fig. 7. The EXAFS oscillations (Fig. 7(a)) indicate that the profiles after lithiation (1st and 2nd) resemble the profile of Ga metal or Li–Ga [15], although it is difficult to distinguish between the profiles of Ga metal and Li–Ga due to broadening and overlap. In order to clarify the local structure around the Ga atom, the curve fitting analysis in *R*-space (Fig. 7(b)) using theoretical phase shifts and backscattering amplitudes calculated by FEFF [16,17] was carried out and selected results are listed in Table 1. The Ga–Ga distances after lithiation (1st and 2nd) are somewhat smaller than that of Ga metal. This would be originated from rearrangements of Ga by the lithiation probably due to the formation of Li–Ga alloys. On the other hand, the spectra after delithiation (1st and 10th) are simi-

Table 1
The selected list of the results of *R*-space curve fitting for the major peaks within 3.0 Å in the Fourier transforms for the k^3-weighted Ga K-EXAFS oscillations. Interatomic distances (*R*) and Debye–Waller factors (σ) around Ga atoms of a Ga_2S_3 electrode before and after the cycle test are listed.

State	Shell	N[a]	R, Å	σ, Å
Initial	Ga–S	4	2.26	0.06
1st lithiation	Ga–Ga	6	2.608	0.13
1st delithiation	Ga–S	4	2.28	0.10
2nd lithiation	Ga–Ga	6	2.627	0.12
10th delithiation[b]	Ga–S	3	2.28	0.11
Ga metal	Ga–Ga	6	2.740	0.16

[a] The coordination number *N*s are fixed to the value of the structure model.
[b] The Fourier transform contains the Ga–Ga pair contribution which reduces the coordination umber of the Ga–S pair.

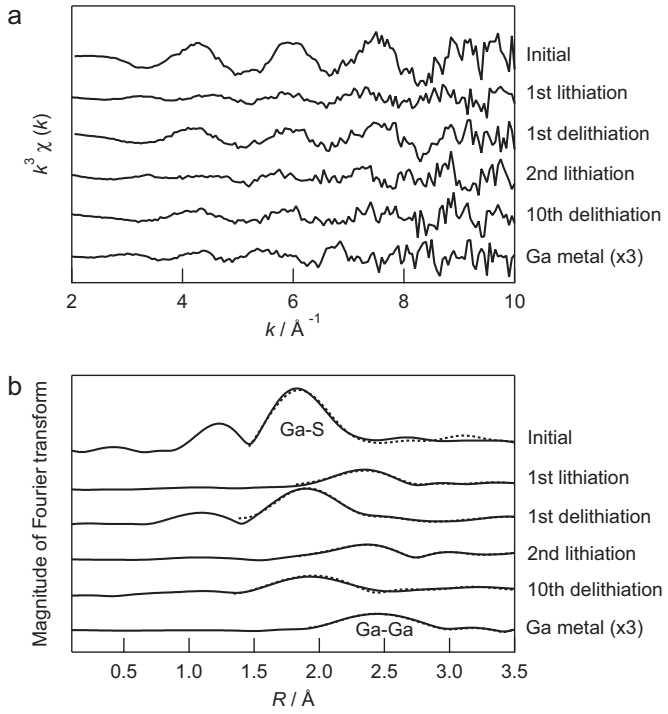

Fig. 7. (a) k^3-weighted EXAFS oscillations of Ga K-edge of a Ga_2S_3 electrode and (b) the corresponding magnitude of Fourier transforms in the transmission mode before and after the cycle test using k^3-weighted EXAFS oscillations with k-range of 1.85–10.7 Å^{-1}. Ga metal was used as a reference. Dashed lines in (b) are the model fit.

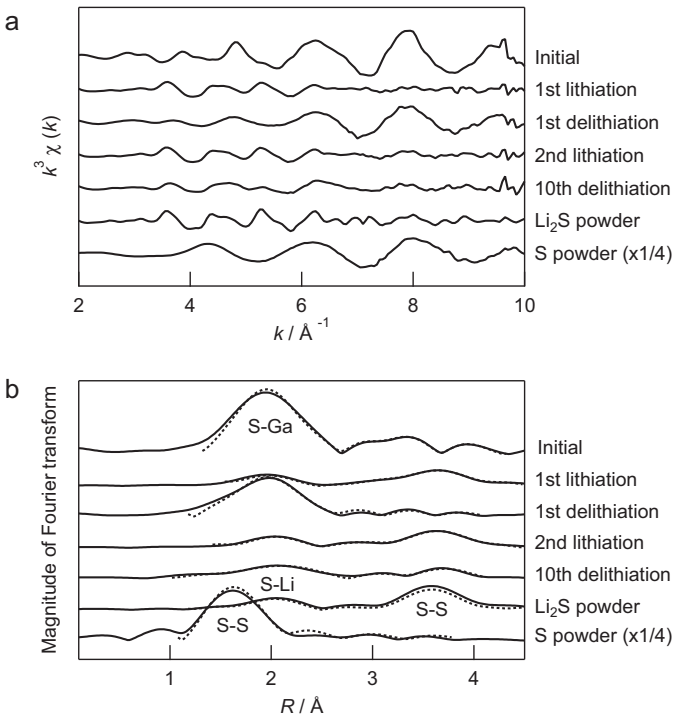

Fig. 9. (a) k^3-weighted EXAFS oscillations of S K-edge of a Ga_2S_3 electrode and (b) the corresponding magnitude of Fourier transforms in the total electron yield mode before and after the cycle test using k^3-weighted EXAFS oscillations with k-range of 1.55–10.0 Å^{-1}. S and Li_2S powders were used as references. Dashed lines in (b) are the model fit.

lar to that before the cycle test (Initial). The relatively larger EXAFS oscillations below $k < 8$ Å^{-1} (Fig. 7(a)) are due to the presence of a low Z atom, S, around the Ga atom. In Table 1, the Ga–S distances after delithiation (1st and 10th) are quite similar to that of Ga_2S_3 before cycle test (Initial). These results suggest that the rearrangement of atoms around Ga occurs reversibly during the lithiation and delithiation. However, as shown in Fig. 7(b), a distinct peak at 1.9 Å in the initial Ga_2S_3 electrode broadens with the cycle number.

Figs. 8 and 9 show the *ex situ* S K-edge XANES and EXAFS spectra of the Ga_2S_3 electrode measured in the total electron yield (TEY) mode. Compared with the Ga K-edge XANES spectra shown in Fig. 6, the S K-edge XANES spectra in Fig. 8 change more significantly during the cycle. The edge position of the Ga_2S_3 electrode (Initial) shifts to a higher energy after the first lithiation. A characteristic peak of Ga_2S_3 at 2472 eV disappears, while a peak at 2476 eV corresponding to Li_2S appears. In the subsequent delithiation, the peak at 2472 eV partially returns, in contrast to disappearance of the peak at 2476 eV. This spectrum is similar to that for Ga_2S_3, but not that for S powder, which reflects the absence of detectable amount of residual S after delithiation. Similar to the first lithiation state, the spectrum after re-lithiation (2nd) is consistent with that of Li_2S. The sample subjected to 10 cycles gives a XANES spectrum that seems to show a superimposition of the lithiation and delithiation states.

The k^3-weighted EXAFS oscillations of the S K-edge of the Ga_2S_3 electrode and the corresponding magnitude of the Fourier transforms are shown in Fig. 9. The selected results of the curve fitting analysis in R-space using theoretical phase shifts and backscattering amplitudes calculated by FEFF are listed in Table 2. The S–Ga distance in Table 2 is the same as the Ga–S distance in Table 1. The behavior of the EXAFS spectra agrees well with that of the XANES spectra in Fig. 8; there is a clear difference in the spectra between

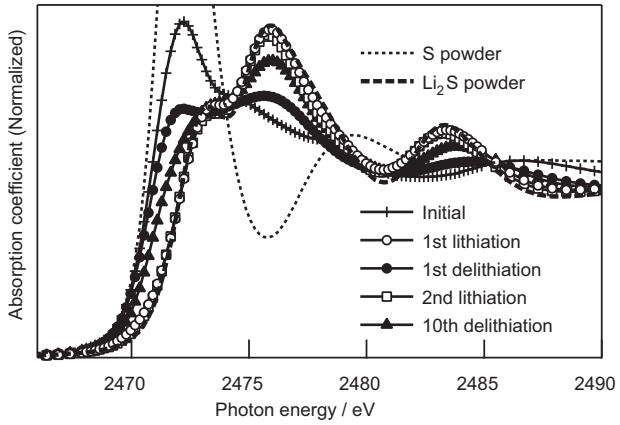

Fig. 8. S K-edge XANES spectra of a Ga_2S_3 electrode in the total electron yield mode before and after the cycle test. S and Li_2S powders were used as references. These spectra were normalized at 2485.5 eV.

Table 2
The selected list of the results of R-space curve fitting for the major peaks within 3.0 Å in the Fourier transforms for the k^3-weighted S K-EXAFS oscillations. Interatomic distances (R) and Debye–Waller factors (σ) around S atoms of a Ga_2S_3 electrode before and after the cycle test are listed.

State	Shell	N[a]	R, Å	σ, Å
Initial	S–Ga	4	2.257	0.091
1st lithiation	S–Li	8	2.454	0.093
1st delithiation	S–Ga	4	2.267	0.093
2nd lithiation	S–Li	8	2.463	0.082
10th delithiation[b]	S–Ga	2	2.285	0.120
	S–Li	4	2.343	0.056
Li_2S powder	S–Li	8	2.472	0.091
S powder	S–S	2	2.047	0.041

[a] The coordination number Ns are fixed to the value of the structure model.
[b] The Fourier transform contains the Li_2S contribution which reduces the coordination umber of the S–Ga pair.

lithiation and delithiation. The spectra after the lithiation (1st and 2nd) are similar to that of Li_2S, which suggests the formation of Li_2S in the electrode. As shown in Table 2, the S–Li distances after the lithiation are also in agreement with that of Li_2S. The presence of a S–Ga bond is reflected in the peak at 1.9 Å in the spectra of the delithiation state (see Fig. 9(b)), the intensity of which decreases with cycling. After 10th delithiation, the presence of a S–Li bond with a S–Ga bond is reasonable by the results of the curve fitting analysis (Table 2). Although the environment of the S atom varies during the cycle test, significant magnitude of signal that could be assigned to the neutral S element was not observed.

We also measured the spectra simultaneously in the partial fluorescence yield (PFY) mode, which reflects the bulk properties of the specimen, in contrast to the TEY mode, which is sensitive to the surface. Generally, the spectra taken in the PFY mode agree with those in the TEY mode. The similarity of the spectra taken in these two methods suggests that the Ga_2S_3 powder homogeneously reacts with Li^+ in the electrolyte during the cycle test.

4. Discussion

Based on the experimental results the reaction mechanism for Ga_2S_3 is believed to mainly consist of two steps:

$$Ga_2S_3 + 6Li^+ + 6e^- \leftrightarrows 2Ga + 3Li_2S \quad 1.0\text{–}2.0\,V \text{ vs. } (Li/Li^+) \tag{1}$$

$$Ga + xLi^+ + xe^- \leftrightarrows Li_xGa \quad < 1.0\,V \text{ vs. } (Li/Li^+) \tag{2}$$

During the reduction process, Ga_2S_3 is lithiated to form Ga metal and Li_2S (reaction (1)). Ga metal is further converted to Li_xGa (Li–Ga) alloy (reaction (2)). Semiconductive Ga_2S_3 is not likely to be lithiated due to its low electronic conductivity. However, Ga metal formed in the early stages of lithiation serves as a conductor, and accelerates the subsequent lithiation of Ga_2S_3. The fact that the impedance decreases during the first lithiation, as shown in Fig. 2, supports this supposition. The formation of Li_2S and Li–Ga alloy is revealed by XRD and XAFS (XANES, EXAFS) analyses. In addition, the measured capacity of the first lithiation is close to the theoretical value. These indicate the almost complete reactions of Ga_2S_3 to Li_2S and Li–Ga alloy. In the reverse process, the delithiated Ga metal induced by reaction (2) reacts with neighboring Li_2S, even though Li_2S is both electronically and ionically resistive [18]. The equilibrium potential of Li_2S/S (2.25 V) [19] exceeds the potential window in the present study, which suggests that the electrochemical reactions are not due to the reaction of Li_2S/S. According to the results of S K-edge EXAFS, the product of the delithiation process must be Ga_2S_3, although the coulomb efficiency is not high enough at the first cycle.

As mentioned in Section 1, Ga_2S_3 is one of the components of lithium-containing sulfide glasses. Ga_2S_3 is added to act as a glass-forming intermediate to extend the range of glass formation by eliminating non-bridging sulfurs [8–10]. This suggests that Ga–S chemical bonds are easily formed when Ga and S atoms are in close proximity to each other, which should be advantageous for the use of Ga_2S_3 as a conversion-type electrode in secondary batteries, where Ga–S bonds are broken and formed during lithiation and delithiation, respectively.

These reactions occur during lithiation/delithiation, which correspond to the two plateaus shown in Fig. 1. With respect to reaction (1), the equilibrium potential calculated from thermodynamic data [20–22] is 1.37 V. This value agrees fairly well with the midpoint between the potentials of higher plateaus during lithiation and delithiation (1.1 V and 1.7 V) shown in Fig. 1. With respect to reaction (2), the electrochemical characteristics below 1.0 V observed in the present study are similar to those for a Li–Ga system reported previously [23,24]. These findings support the notion that reactions (1) and (2) occur at the higher and lower potentials, respectively, during lithiation and delithiation. The reaction mechanism of the Ga_2S_3 electrode is similar to that of the Al_2S_3 electrode [7].

As shown in Fig. 3, the capacity decreases more rapidly in the initial five cycles. The potential profiles (Fig. 1) suggest that this decrease is mainly due to delithiation. While the plateau region at a lower potential becomes smaller within only a few cycles that at a higher potential becomes smaller gradually. If we consider the reaction mechanism, the degradations within a few cycles and after 5 cycles can be attributed to low-efficiency Li extractions from Li–Ga alloy and the accumulation of electrochemically inactive Li_2S, respectively. In fact, the radial distribution after the 10th delithiation (Fig. 9(b)) can be regarded as a superimposition of small amounts of non-reacted Ga_2S_3 and accumulated inactive Li_2S. The irreversibility of the oxidation state of Ga in the early stage of the cycle test is confirmed by the Ga K-edge XANES analysis. Tarascon and co-workers [23] reported that, in a Li–Ga system, cell performance is reduced due to volume variations that cause a decrease in the mechanical coherence of the electrode. The degradation behavior they reported in the Li–Ga system is similar to our data below 1.0 V. Moreover, while an almost reversible reaction between Ga_2S_3 and Li_2S (reaction (1)) occurs in the early stage of the cycle test, the poor electronic conductivity of Li_2S leads to an irreversible reaction. These phenomena may be responsible for the degradation of the Ga_2S_3 electrode.

If we wish to improve cycle retention, it is important to suppress crystal growth and the isolation of products. *Ex situ* XRD analysis shows that after lithiation, a Li_2S peak is apparently observed while the Ga_2S_3 phase is hardly observed after delithiation. The limitation of crystal growth and the isolation of electrochemically inactive Li_2S phase may improve the electronic conductivity between particles, which would lead to the good cycle durability. Studies on the preparation of an appropriate Ga_2S_3 electrode are currently underway.

5. Summary

The electrochemical characteristics of Ga_2S_3 for use in lithium secondary batteries were investigated using a galvanostatic cycle. The specific capacity of Ga_2S_3 at the initial delithiation is, in practice, more than twice as high as that of a conventional graphite anode. Cycle degradation is mainly due to delithiation. The suppression of crystal growth in the Li_2S and Li–Ga phases in both the surface and core of the electrode may lead to superior capacity retention.

Acknowledgements

The authors are grateful to their colleagues at the Research Institute for Ubiquitous Energy Devices for their helpful suggestions and stimulating discussions, especially Dr. N. Fujiwara, Dr. T. Ioroi, Dr. Z. Siroma and Dr. S. Yamazaki. We also wish to thank Ms. J. Hirai and Ms. Okumura for their helpful assistance. S K-edge XAFS analyses were performed under a nanotechnology network project at Ritsumeikan University.

References

[1] X.L. Ji, K.T. Lee, L.F. Nazar, Nat. Mater. 8 (2009) 500–506.
[2] R. Fong, J.R. Dahn, C.H.W. Jones, J. Electrochem. Soc. 136 (1989) 3206–3210.
[3] A. Débart, L. Dupont, R. Patrice, J.M. Tarascon, Solid State Sci. 8 (2006) 640–651.
[4] T. Takeuchi, H. Sakaebe, H. Kageyama, T. Sakai, K. Tatsumi, J. Electrochem. Soc. 155 (2008) A679–A684.
[5] Y. Kim, H. Hwang, K. Lawler, S.W. Martin, J. Cho, Electrochim. Acta 53 (2008) 5058–5064.
[6] B.T. Hang, T. Ohnishi, M. Osada, X.X. Xu, K. Takada, T. Sasaki, J. Power Sources 195 (2010) 3323–3327.

[7] H. Senoh, T. Takeuchi, H. Kageyama, H. Sakaebe, M. Yao, K. Nakanishi, T. Ohta, T. Sakai, K. Yasuda, J. Power Sources 195 (2010) 8327–8330.
[8] M. Yamashita, H. Yamanaka, H. Wakabayashi, Solid State Ionics 89 (1996) 299–304.
[9] R. Kanno, T. Hata, Y. Kawamoto, M. Irie, Solid State Ionics 130 (2000) 97–104.
[10] J. Saienga, Y. Kim, B. Campbell, S.W. Martin, Solid State Ionics 176 (2005) 1229–1236.
[11] K. Nakanishi, T. Ohta, J. Phys. Condens. Matter 21 (2009) 104214.
[12] J. Goodyear, W.J. Duffin, G.A. Steigmann, Acta Cryst. 14 (1961) 1168–1170.
[13] E. Zintl, A. Harder, B. Dauth, Z. Elektrochem. 40 (1934) 588–593.
[14] E. Zintl, G. Brauer, Z. Physik, Chemistry B20 (1933) 245–271.
[15] H. Hwang, M.G. Kim, J. Cho, J. Phys. Chem. C 111 (2007) 1186–1193.
[16] J.J. Rehr, J. Mustre de Leon, S.I. Zabinsky, R.C. Albers, J. Am. Chem. Soc. 113 (1991) 5135–5140.
[17] J. Mustre de Leon, J.J. Rehr, S.I. Zabinsky, R.C. Albers, Phys. Rev. B 44 (1991) 4146–4156.
[18] M.N. Obrovac, J.R. Dahn, Electrochem. Solid State Lett. 5 (2002) A70–A73.
[19] T. Takeuchi, H. Sakaebe, H. Kageyama, H. Senoh, T. Sakai, K. Tatsumi, J. Power Sources 195 (2010) 2928–2934.
[20] A.S. Gates, J.G. Edwards, J. Phys. Chem. 82 (1978) 2789–2796.
[21] Kagaku-Binran, The Electrochemical Society of Japan, 5th ed., Maruzen, Tokyo, 2000.
[22] J.G. Speight (Ed.), Lange's Handbook of Chemistry, 16th ed., McGraw-Hill, New York, 2005.
[23] J. Saint, M. Morcrette, D. Larcher, J.M. Tarascon, Solid State Ionics 176 (2005) 189–197.
[24] K.T. Lee, Y.S. Jung, T. Kim, C.H. Kim, J.H. Kim, J.Y. Kwon, S.M. Oh, Electrochem. Solid State Lett. 11 (2008) A21–A24.